Journal of Applied Physics

Formation of nitrogen-vacancy centers in 4H-SiC and their near infrared photoluminescence properties

Cite as: J. Appl. Phys. **126**, 083105 (2019); https://doi.org/10.1063/1.5099327
Submitted: 09 April 2019 . Accepted: 27 July 2019 . Published Online: 23 August 2019

Shin-ichiro Sato (佐藤 真一郎), Takuma Narahara (楢原 拓真), Yuta Abe (阿部 裕太), Yasuto Hijikata (土方泰斗), Takahide Umeda (梅田 享英), and Takeshi Ohshima (大島 武)

ARTICLES YOU MAY BE INTERESTED IN

Energy levels and charge state control of the carbon antisite-vacancy defect in 4H-SiC
Applied Physics Letters **114**, 212105 (2019); https://doi.org/10.1063/1.5098070

Identification of divacancy and silicon vacancy qubits in 6H-SiC
Applied Physics Letters **114**, 112107 (2019); https://doi.org/10.1063/1.5083031

Bright single photon sources in lateral silicon carbide light emitting diodes
Applied Physics Letters **112**, 231103 (2018); https://doi.org/10.1063/1.5032291

© 2019 Author(s).

Journal of Applied Physics ARTICLE scitation.org/journal/jap

Formation of nitrogen-vacancy centers in 4H-SiC and their near infrared photoluminescence properties

Cite as: J. Appl. Phys. **126**, 083105 (2019); doi: 10.1063/1.5099327
Submitted: 9 April 2019 · Accepted: 27 July 2019 ·
Published Online: 23 August 2019

View Online
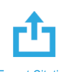
Export Citation

CrossMark

Shin-ichiro Sato (佐藤 真一郎),[1,a)] Takuma Narahara (楢原 拓真),[1,2] Yuta Abe (阿部 裕太),[1,3] Yasuto Hijikata (土方 泰斗),[2] Takahide Umeda (梅田 享英),[3] and Takeshi Ohshima (大島 武)[1,3]

AFFILIATIONS

[1]Quantum Beam Science Research Directorate, National Institutes for Quantum and Radiological Science and Technology, 1233 Watanuki, Takasaki, Gunma 370-1292, Japan
[2]Graduate School of Science and Engineering, Saitama University, 255 Shimo-ohkubo, Sakura-ku, Saitama, Saitama 338-8570, Japan
[3]Tsukuba Research Center for Energy Materials Science, University of Tsukuba, 1-1-1 Tennodai, Tsukuba, Ibaraki 305-8577, Japan

[a)]**Author to whom correspondence should be addressed:** sato.shinichiro2@qst.go.jp

ABSTRACT

$N_CV_{Si}^-$ centers in SiC [nitrogen-vacancy (NV) centers], which produce near-infrared (NIR) photoluminescence (PL) at room temperature, is expected to have applications as quantum sensors for *in vivo* imaging and sensing. To realize quantum sensing using NV centers, clarification of the formation mechanism as well as control of the high-density formation is necessary. This paper reports a comprehensive investigation on the NIR-PL properties originating from NV centers in high purity semi-insulating and nitrogen (N) contained 4H-SiC substrates formed by ion beam irradiation and subsequent thermal annealing. It is shown that NV centers are exclusively formed by the contained N as impurities rather than the implanted N, and also the heavier ion irradiations induce the NV center formation effectively than the lighter ion irradiations. The study on thermal annealing at different temperatures reveals that the optimal temperature is 1000 °C. From the results of temperature dependence on the PL intensity, it is shown that little thermal quenching of the PL intensity appears at room temperature and the PL signal is collected even at 783 K. The formation mechanism of NV centers is also discussed based on the obtained results.

Published under license by AIP Publishing. https://doi.org/10.1063/1.5099327

I. INTRODUCTION

Defects and color centers in wide-gap semiconductors, of which the spin state can be optically controlled, are of strong interest because of their potential for applications in quantum computing (qubit)[1–4] and sensing.[5–8] The negatively charged nitrogen-vacancy (NV) center in diamond has been proven to be a prominent solid-state qubit which can be operated at room temperature (RT),[3,9,10] and the great success of NV centers in diamond has also stimulated further exploration of optically active spin-carrying defects. Silicon carbide (SiC) is one of the attractive host materials for quantum sensing and metrology because the crystal growth technology, in addition to the device fabrication technology, are well developed and SiC-based electrically driven quantum sensors are feasible.[11,12] It has been demonstrated that silicon vacancies (V_{Si}^-)[13–18] and divacancies ($V_{Si}V_C$ or simply VV)[19–26] could serve as controllable spin states with sharp zero-phonon lines (ZPLs).

Recently, $N_CV_{Si}^-$ centers in SiC, i.e., negatively charged pairs of silicon vacancy and a nitrogen atom on an adjacent carbon site, have been proposed as another optically active defect with an electronic structure strongly resembling that of NV centers in diamond.[27–31] ZPLs of the absorption between the $^3A_2$ ground state and the ^3E excited state are located at around 1200 nm, much longer than that of diamond-NV centers (638 nm). This optical property is advantageous for *in vivo* imaging and sensing, since the near-infrared (NIR) light can penetrate biological tissues such as skin and blood more efficiently than visible light.[32,33] Also, unlike VVs, $N_CV_{Si}^-$ centers produce luminescence and possibly their spin

Published under license by AIP Publishing.

states can be manipulated at room temperature (RT), which are the essential properties for life science applications. In addition, operation at higher temperatures than RT is required for quantum sensing applications under harsh environments such as diagnostics of power electronics and vectorized magnetometer in space.[34] For example, devices mounted on spacecrafts for Venus exploration missions must withstand temperatures of up to 460 °C, the Venusian surface temperature. $N_CV_{Si}^-$ centers in SiC hold the promise of quantum sensors which can meet these various needs. Here, "$N_CV_{Si}^-$ centers in SiC" is represented as "NV centers" for simplicity unless otherwise noted.

Unfortunately, the optical spin-state manipulation [e.g., optically detected magnetic resonance (ODMR)] of NV centers has not been demonstrated to date. One of the reasons is that the formation mechanism has been less well understood and the optimum fabrication procedure has not yet been established. For quantum sensing based on optical spin-state manipulation, a higher density of NV centers is crucial to improve sensitivity without increasing the volume, maintaining the high spatial resolution achievable. Not having been observed in any as-grown SiC materials, NV centers could be introduced only by using energetic particle irradiation and subsequent thermal annealing. For example, von Bardeleben *et al.* have reported that NV centers were formed by 12 MeV proton irradiation at the fluence of $1 \times 10^{16}\,\mathrm{cm}^{-2}$ and subsequent 900 °C annealing in n-type 4H-SiC.[31] Effects of radiation species, fluence, and irradiation temperature on the formation of NV centers should be systematically investigated. High energy electrons and protons produce point defects sparsely in crystals, whereas heavy ions produce cascade damage, i.e., localized dense defect regions, in addition to point defects. Thus, differences among irradiated ion species reflect the mechanism of NV center formation. Moreover, thermal annealing conditions after irradiation should be optimized, since sufficient vacancy diffusion is not expected at low temperature, whereas different types of complex defects may be formed at high temperature. It is also interesting to explore whether nitrogen (N) as impurities or implanted N dominates NV center formation. In this study, we systematically investigated NIR photoluminescence (PL) properties of ion irradiated 4H-SiC in order to understand the NV center formation mechanism and to control it. Two types of 4H-SiCs, n-type 4H-SiC with the nitrogen concentration of 9×10^{18} cm^{-3} and HPSI (high purity semi-insulating) 4H-SiC, were used in this study.

II. EXPERIMENTAL

Samples used in this study were n-type 4H-SiC and HPSI (high purity semi-insulating) 4H-SiC substrates. Here, these samples are represented by N-4H-SiC and HPSI-4H-SiC, respectively. The N concentrations of N-4H-SiC and HPSI-4H-SiC were determined to be $9 \times 10^{18}\,\mathrm{cm}^{-3}$ and $3 \times 10^{15}\,\mathrm{cm}^{-3}$ by Secondary Ion Mass Spectroscopy (SIMS). The samples were irradiated with 240 keV-H (hydrogen), 2 MeV-N (nitrogen), 4 MeV-Si (silicon), and 7 MeV-I (iodine) ion beams at different fluences at RT. These ion beam energies were chosen so that radiation defects were introduced at the depth of about 1.5 μm from the surface. The average ion beam fluxes were $2.6 \times 10^{12}\,\mathrm{cm}^{-2}\,\mathrm{s}^{-1}$ for 240 keV-H, $1.9 \times 10^{11}\,\mathrm{cm}^{-2}\,\mathrm{s}^{-1}$ for 2 MeV-N, $1.0 \times 10^{11}\,\mathrm{cm}^{-2}\,\mathrm{s}^{-1}$ for 4 MeV-Si, and $5.2 \times 10^{10}\,\mathrm{cm}^{-2}\,\mathrm{s}^{-1}$ for 7 MeV-I. Figure 1 shows the depth profiles of radiation defects (vacancies) formed by these ion beams, calculated by Monte Carlo Simulation Code, TRIM.[35] The mass density of $3.21\,\mathrm{g\,cm}^{-3}$ and the displacement threshold energies of 25 eV for Si and 21 eV for C were used for the calculation,[36] although slightly different values have also been reported.[37,38] All the ion implantations were performed at the Takasaki Advanced Radiation Research Institute, National Institutes for Quantum and Radiological Science and Technology (QST). After ion irradiation, all the samples were thermally annealed under Ar atmosphere (1 atm) using an infrared furnace. The furnace temperature rose to a set temperature in 1 min, then kept at the set temperature for 30 min, and was then naturally cooled down to RT for about 15 min.

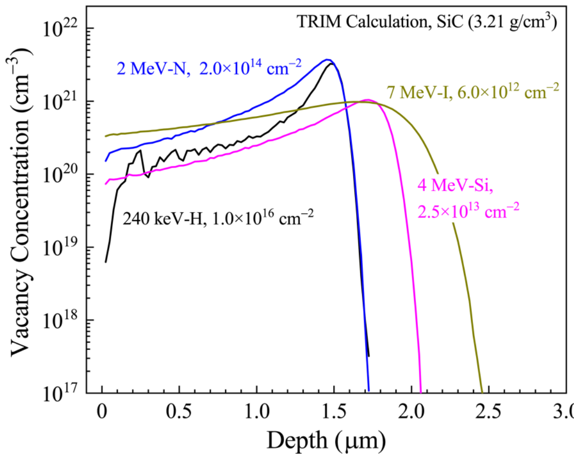

FIG. 1. Vacancy concentration profiles in SiC ($3.21\,\mathrm{g\,cm}^{-3}$) induced by ion beams used in this study, calculated by TRIM.[35] Lines in black, blue, pink, and dark yellow denote 240 keV-H, 2 MeV-N, 4 MeV-Si, and 7 MeV-I, respectively. Fluences, which the highest PL intensity was obtained at, are shown in this figure (see Fig. 7).

NIR-PL properties at the irradiated region in the samples at RT and 80 K were investigated using HORIBA LabRAM HR Evolution (micro-PL measurement system). The excitation laser wavelength was either 785 nm or 1064 nm. PL ranging from 850 nm to 1500 nm from the samples was collected with an objective lens (numerical aperture, NA is 0.90 at RT and 0.50 at 80 K) and detected by an InGaAs array detector. The laser spot diameter estimated from the used objective lens was 1.1 μm (785 nm laser, RT), 1.9 μm (785 nm laser, 80 K), 1.4 μm (1064 nm laser, RT), and 2.6 μm (1064 nm laser, 80 K).

III. RESULTS AND DISCUSSION

A. Comparison of 785 nm and 1064 nm excitations

Figure 2 shows NIR-PL spectra at 80 K of HPSI- and N-4H-SiC samples through 785 nm and 1064 nm excitations. The samples were irradiated with 2 MeV-N ions at a fluence of $2.0 \times 10^{14}\,\mathrm{cm}^{-2}$ and subsequently thermally annealed at 1000 °C for 30 min under Argon (Ar) atmosphere after irradiation. The peak

Published under license by AIP Publishing.

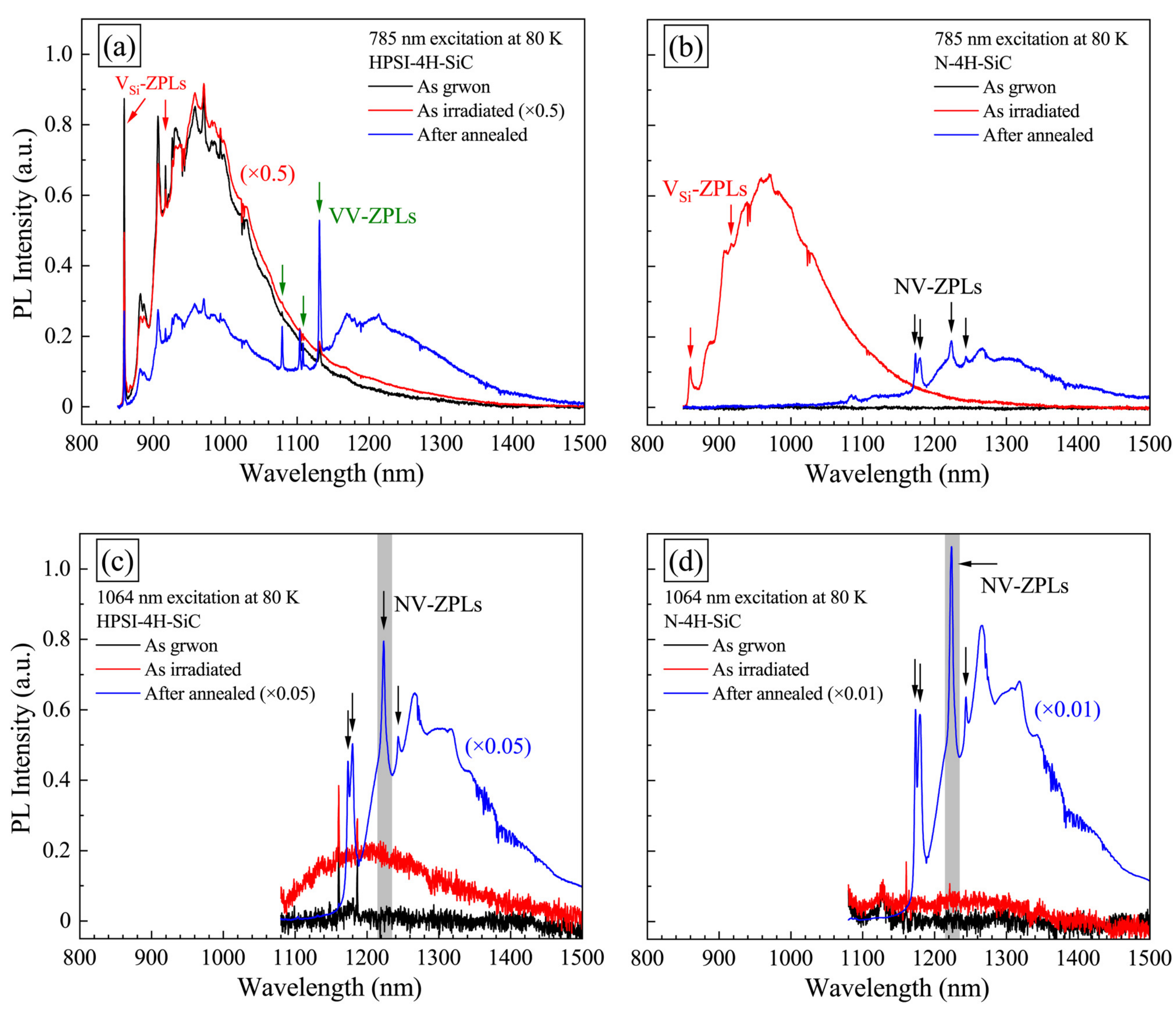

FIG. 2. Typical NIR-PL spectra of HPSI- and N-4H-SiCs at 80 K: (a) HPSI-4H-SiCs excited by 785 nm, (b) N-4H-SiCs excited by 785 nm, (c) HPSI-4H-SiCs excited by 1064 nm, and (d) N-4H-SiCs excited by 1064 nm. Black, red, and blue lines show as-grown, as-irradiated with 2 MeV-N at the fluence of $2.0 \times 10^{14}\,\mathrm{cm}^{-2}$, and after thermal annealing at 1000 °C for 30 min in Ar atmosphere, respectively. Arrows in the figure indicate NV-ZPLs (black), VV-ZPLs (green), and V_{Si}-ZPLs (red). Note that the red line in (a) and the blue lines in (c) and (d) are scaled by a constant factor of 0.5, 0.05, and 0.01, respectively, to clearly show the spectra. Shaded zones in (c) and (d) denote integration ranges of the PL intensities used in Fig. 6.

concentration of radiation induced defects appears at 1.5 μm in depth due to 2 MeV-N irradiation and PL spectra near the surface region were obtained. The PL intensity as a function of depth direction revealed that all luminescent centers were formed near the surface and no significant diffusion after thermal annealing was observed. Also, planar distribution of the PL intensity was almost uniform for all samples.

In the case of HPSI-4H-SiC samples, a broad peak centered at 950 nm appeared by 785 nm excitation [Fig. 2(a)]. This broad peak is attributable to phonon side bands (PSBs) of V_{Si}^{-}s.[17] Two ZPLs of V_{Si}^{-}s, which are indicated by red arrows in (a), also appeared with the broad PSBs. After 2 MeV-N irradiation, the PL intensity from V_{Si}^{-} increased about twofold due to an increase in density of V_{Si}^{-}. However, the broad peak centered at 950 nm was reduced after 1000 °C thermal annealing, and a broad peak centered at 1200 nm in addition to four sharp peaks at around 1100 nm newly appeared. They are attributable to four ZPLs of VVs and their PSBs.[26,29] This means that the density of V_{Si}^{-} was reduced and VVs were formed due to 1000 °C thermal annealing. On the other hand, neither PL signal from V_{Si}^{-}s nor VVs appeared when excited by 1064 nm.

Published under license by AIP Publishing.

A broad peak centered at 1300 nm and four sharp peaks at around 1200 nm appeared after 1000 °C thermal annealing [Fig. 2(c)]. They are attributable to four ZPLs of NV centers and their PSBs.[26,29] Prior to thermal annealing, the two sharp peaks observed at 1160.6 nm and 1186.5 nm were assigned to be Raman scattering of the E_2 planar optical (PO) and the A_1 longitudinal optical (LO) phonons, respectively.[39] The difference of PL spectra between 785 nm and 1064 nm excitations suggests that NV centers can be effectively excited by 1064 nm, whereas VVs can be excited by 785 nm. In the case of N-4H-SiCs, no PL was observed from as-grown samples and the PL originating from V_{Si}^{-}s appeared after 2 MeV-N irradiation when excited by 785 nm. After 1000 °C thermal annealing, the PL originating from NV centers appeared by exciting at both 785 nm and 1064 nm. No PL from VVs was observed by exciting at either wavelength. Also, only the E_2 PO phonon mode appeared at 1160.6 nm in the N-4H-SiCs because the LO phonon mode is reduced by the coupling between phonons and plasmons.[40,41]

Wavelengths of the observed ZPLs, which appeared in the PL spectra at 80 K by both 785 nm and 1064 nm excitations, are summarized in Table I. Two V_{Si}^{-}-ZPLs, four VV-ZPLs, and four NV^{-}-ZPLs have previously been identified by other groups[17,26,29] and we identified ZPLs in Fig. 2 by comparing these previous values. Two V_{Si}^{-}-ZPLs have been labeled as V1 and V2, which have been assigned to be V_{Si}^{-} in the horizontal (*h*) and cubic (*k*) sites of 4H-SiC lattice, respectively.[14] However, contradictory results have also been reported.[42] There are four different VV-ZPLs depending on the configuration of V_C and V_{Si}. They have been identified as *kh* (V_C at *k* site and V_{Si} at *h* site, the same hereinafter), *hk*, *hh*, and *kk* sites in descending order of ZPL energy. *kh* and *hk* sites are the basal configurations, and *hh* and *kk* sites are the axial configurations. Four NV-ZPLs have also been identified as *hk*, *hh*, and *kk* sites in descending order of ZPL energy as with the case of VVs[27,29] In the case of HPSI-4H-SiC irradiated with 2 MeV-N ions, two V_{Si}-ZPLs and four VV-ZPLs appeared by 785 nm excitation, whereas four NV-ZPLs dominantly appeared by 1064 nm excitation. A similar trend has also previously been reported.[29] We believe that VV-ZPLs from the *hh* and *kk* sites overlapped and the strong peak at 1130.9 nm appeared by 785 nm excitation. On the contrary, only four NV-ZPLs appeared in the case of N-4H-SiCs after thermal annealing. Neither V_{Si}-ZPLs nor VV-ZPLs have been clearly identified. Slight discrepancies of the obtained ZPL wavelengths compared to previous reports are thought to be due to an effect of lattice strains induced by ion irradiations and thermal annealing.

Interestingly, no VV-ZPL and only NV-ZPLs were observed in the N-4H-SiC samples. This indicates that NV centers were more preferentially formed than VVs This is due to the lower formation energy of NV centers than that of VVs[43] Also, if VVs are created, they are immediately transferred to NV centers by the reaction with nitrogen-carbon split interstitial, $(NC)_C^{+}$: $(NC)_C^{+} + V_C V_{Si} + 2e^{-} \rightarrow N_C V_{Si}^{-}$ (to be discussed later).[44] On the other hand, VVs were still formed in the HPSI-4H-SiC samples and were excited preferentially by 785 nm, but not excited at 1064 nm. Only NV centers were excited by 1064 nm. It has been clarified that the excitation efficiency of VVs dropped above 980 nm.[26] However, only PL from NV centers were observed at RT

TABLE I. Summary of ZPLs (nm) observed in Fig. 2. The nature of ZPLs was identified by the comparison to previous reports by other research groups[17,26,29] listed in the table. Weakly observed ZPLs are shown in italics. Note that *hh* and *kk* denote the axial configuration of VVs and *kh* and *hk* are the basal configurations of VVs (see text in detail).

Sample	Laser (nm)	Temperature (K)	V_{Si}^{-} (V1)	V_{Si}^{-} (V2)	VV (*kh*)	VV (*hk*)	VV (*hh*)	VV (*kk*)	NV (*kh*)	NV (*hk*)	NV^{-} (*hh*)	NV^{-} (*kk*)	Unidentified
HPSI-4H-SiC	785	80	859.1	916.1	1079.1	1108.3	1130.9		*1173.4*	*1180.2*			1103.6
	1064	80							1173.7	1179.9	1223.3	1243.6	
N-4H-SiC	785	80	860.1	916.4					1173.3	1179.9	1223.5	1243.6	*1084.1* *1089.9*
	1064	80							1173.7	1179.7	1223.7	1243.8	
Magnusson *et al.*[26]	811, 930	3.5	861.6		1078.5	1107.6	1130.5	1132.0	1176.4	1180.0	1223.2	1242.8	
Zargaleh *et al.*[29]	715-1000	10			1078.1	1108.0	1132.2	1132.2	1179.6	1222.7	1241.0	1242.3	
Fuchs *et al.*[17]	785	5	861.4	916.3									

Published under license by AIP Publishing.

in both the HPSI- and N-4H-SiC samples because the PL from VVs was negligibly weak at RT. Figure 3 shows the PL spectra of HPSI- and N-4H-SiC samples at RT. Unlike PL spectra at 80 K, only broad peaks originated from PSBs and no ZPLs appeared. Sharp peaks observed at 1088.2 nm, 1160.6 nm, and 1186.4 nm, when excited by 1064 nm, were assigned to be Raman scatterings of the E_2 planar acoustic (PA), the E_2 PO, and the A_1 LO phonons, respectively.[39] Again, the A_1 LO phonon modes did not appear in the N-4H-SiCs because of the phonon-plasmon coupling. The broad peaks centered at 950 nm and 1300 nm are attributable to PL from V_{Si}^- and NV centers, respectively. These variations were in agreement with the variation at 80 K. Figure 4 shows the PL integrated intensity as a function of the distance between the focal point and the sample surface at RT. All luminescent centers were formed near the surface and no significant diffusion after thermal annealing was observed. The similar trend was also found at 80 K and at 1064 nm excitation.

The PL intensity at different laser power densities was measured to investigate the excitation efficiency of NV centers. Figure 5 shows the PL integrated intensity as a function of excitation laser power density. The PL intensity increased monotonically with increasing excitation power density and no obvious saturation

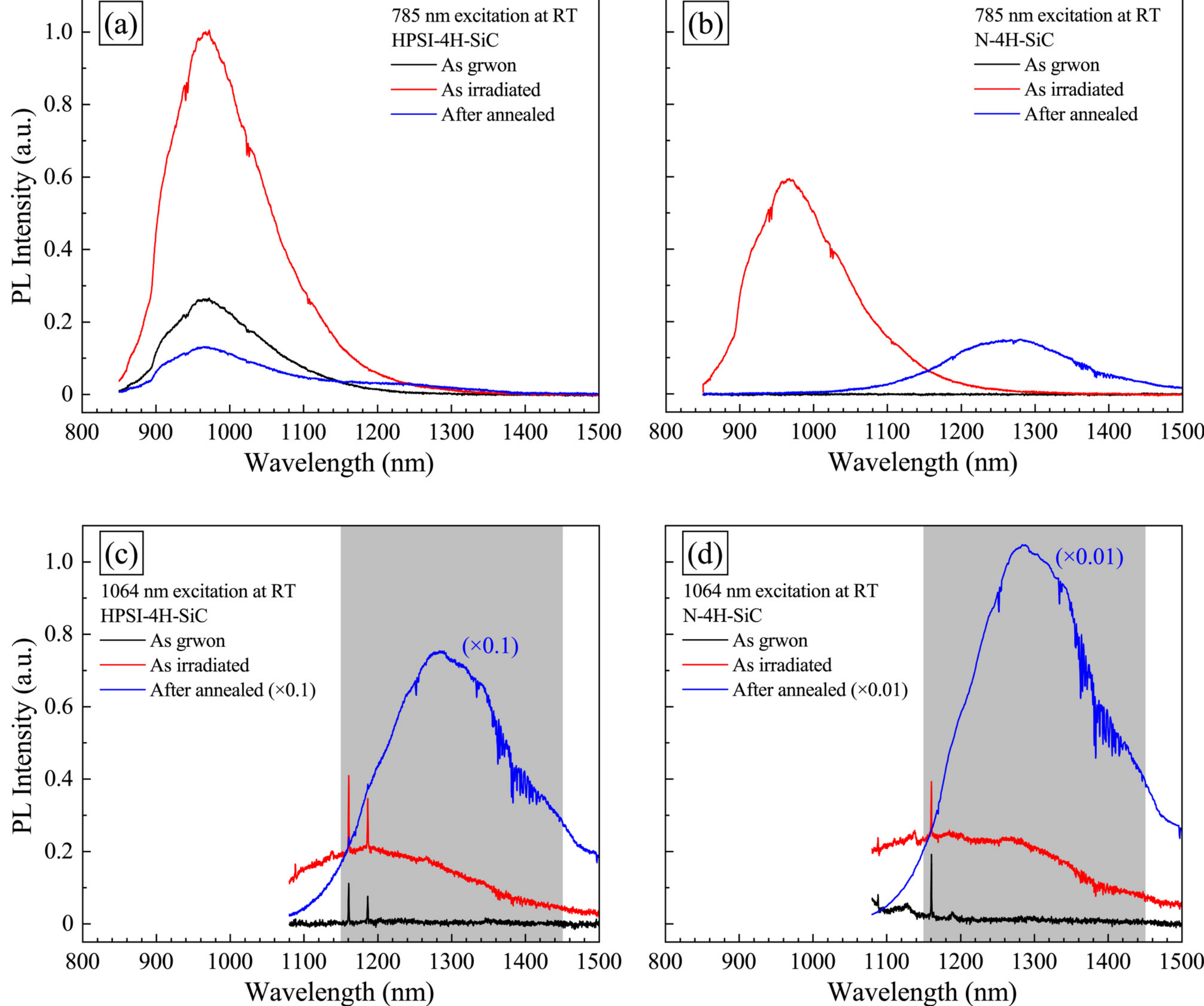

FIG. 3. Typical NIR-PL spectra of HPSI- and N-4H-SiCs at RT: (a) HPSI-4H-SiCs excited by 785 nm, (b) N-4H-SiCs excited by 785 nm, (c) HPSI-4H-SiCs excited by 1064 nm, and (d) N-4H-SiCs excited by 1064 nm. Black, red, and blue lines show as-grown, as-irradiated with 2 MeV-N at the fluence of 2.0×10^{14} cm^{-2}, and after thermal annealing at 1000 °C for 30 min in Ar atmosphere, respectively. Note that the blue lines in (c) and (d) are scaled by a constant factor of 0.1 and 0.01, respectively, to clearly show the spectra. Shaded zones in (c) and (d) denote integration ranges of the PL intensities used in Figs. 4, 5, 6, 7, and 10.

Published under license by AIP Publishing.

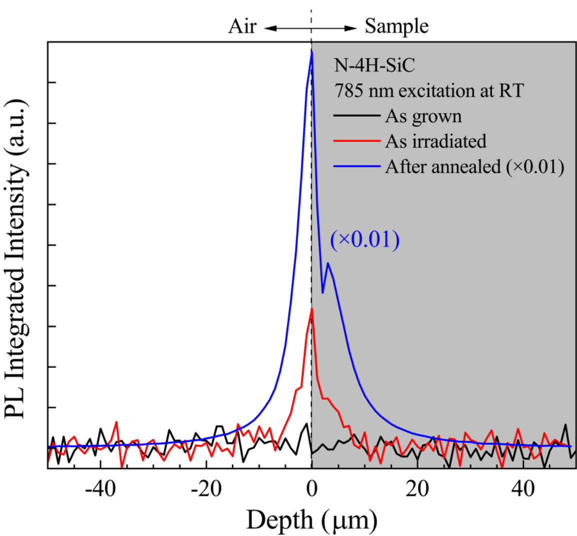

FIG. 4. The PL integrated intensity (1150–1450 nm) of N-4H-SiC samples as a function of the distance between the focal point and the sample surface. The PL measurement was performed through 785 nm excitation at RT. Black, red, and blue lines denote the results of as-grown, as-irradiated with 2 MeV-N at the fluence of 2.0×10^{14} cm^{-2}, and after 1000 °C thermal annealing for 30 min in Ar atmosphere, respectively. "Depth = 0" means the surface. The value is negative when the focal point is above the surface (air) and positive when below the surface. Note that the blue line is scaled by a constant factor of 0.01 to clearly show the data.

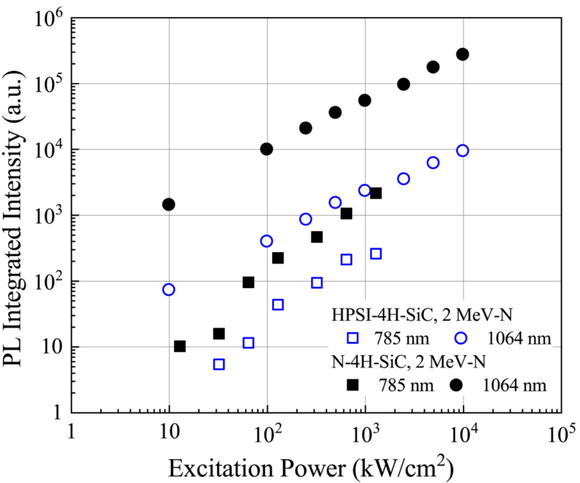

FIG. 5. The PL integrated intensity at RT (1150–1450 nm) as a function of excitation laser power density (785 nm and 1064 nm). Black closed and blue open symbols denote the N- and HPSI-4H-SiCs irradiated with 2 MeV-N at the fluence of 2.0×10^{14} cm^{-2}, respectively.

behaviors were observed in all cases within the power densities investigated in this study. The PL intensity by 1064 nm excitation was more than 10 times higher than 785 nm excitation, suggesting that 1064 nm laser excites NV centers more efficiently than 785 nm laser. The similar trend was also found at 80 K. According to the theoretical calculation by Weber *et al.*,[2] the absorption energy of NV centers in 4H-SiC is 1.15 eV, which is fairly close to the photon energy of 1064 nm (1.165 eV). On the other hand, in the case of 785 nm excitation, we speculate that the photon energy (1.58 eV) is high enough to induce charge transfer to valence/conduction band and other defects, resulting in the reduction of PL intensity. Charge state transfer has been reported in other defects such as diamond-NV centers and VVs in 4H-SiC.[19,20,45]

B. Thermal annealing temperature dependence

The N- and HPSI-4H-SiC samples were irradiated with 2 MeV-N ions at a fluence of 2.0×10^{14} cm^{-2} and thermally annealed at temperatures from 700 °C to 1100 °C for 30 min under Ar atmosphere. The excitation wavelength of PL measurement was 1064 nm. Figure 6 shows the results of N- and HPSI-4H-SiC samples, respectively. The ordinate is the relative PL integrated intensity from 1150 nm to 1450 nm at RT and from 1215 to 1235 nm at 80 K (NV-ZPL at *hh* site), which are represented by shaded zones in Figs. 2 and 3, although both data showed the same trend. In the case of N-4H-SiC, the PL integrated intensity showed the highest at 1000 °C and was rather reduced at above 1000 °C. It appears that N-related complex defects like $(N_C)_xV_{Si}$ are preferentially formed at above 1000 °C[43,44] because of the high N-impurity concentration ($[N] = 9 \times 10^{18}$ cm^{-3}), resulting in the reduction of the NV center concentration. It is known that higher annealing temperatures than 1500 °C are required to annihilate the N-related

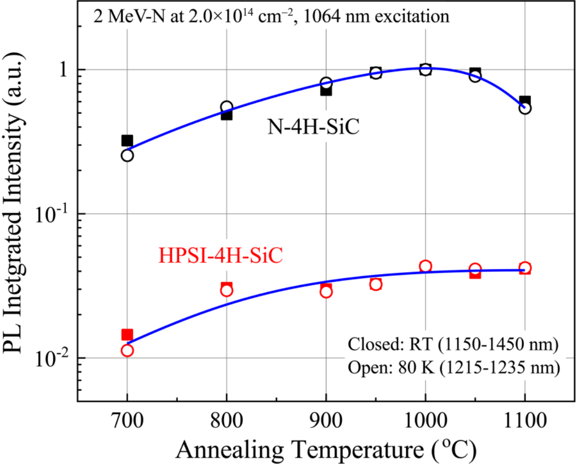

FIG. 6. The PL integrated intensity as a function of thermal annealing temperature measured at RT (closed squares) and 80 K (open circles). Black and red symbols denote the results of N- and HPSI-4H-SiCs irradiated with 2 MeV-N at the fluence of 2.0×10^{14} cm^{-2}, respectively. Thermal annealing was performed for 30 min in Ar atmosphere after irradiation. The ordinate is the PL integrated intensity (RT: 1150–1450 nm, 80 K: 1215–1235 nm) and is normalized by the value of N-4H-SiC at 1000 °C. Solid lines in blue are drawn to guide the eye.

Published under license by AIP Publishing.

complex defects and to obtain perfect recovery of crystallinity.[46,47] On the other hand, the PL integrated intensity increased with increasing temperature and showed a saturation trend above 1000 °C in the case of HPSI-4H-SiC. It should be noted that relatively larger fluctuation of PL intensity appeared in the HPSI-4H-SiC because of their lower PL intensity. Finally, additional thermal annealing for 30 min at the same temperatures as Fig. 6 was performed for all the samples, although no significant change was observed.

According to theoretical calculations, there are mainly two processes to form NV centers. One is the simple process: $N_C^+ \pm V_{Si}^- \pm e^- \rightarrow N_CV_{Si}^-$[43] and the other is the multiple process via $(NC)_C^+$ split interstitial and V_CV_{Si}: $(CC)_C \pm N_C^+ \rightarrow (NC)_C^+$ and $(NC)_C^+ \pm V_CV_{Si} \pm 2e^- \rightarrow N_CV_{Si}^-$.[44] Here, the former and latter processes are represented by processes (1) and (2), respectively. Defect kinetics of V_{Si}^- is thought to play an important role in the process (1). Although the annealing occurs in several stages at 150 °C, 350 °C, and 750 °C, more than 1450 °C is required to be annealed completely.[48] This annealing behavior is explained by the formation of stable nitrogen-vacancy complexes. In our study, both the reduction of V_{Si}^- and the formation of NV centers appeared due to thermal annealing at 700–1100 °C. This fact may indicate that the direct formation process (1) contributed to the creation of NV centers. However, interstitial carbons (I_C) are more mobile than vacancies and form $(CC)_C$ and then form NV centers via the process (2). We believe that process (2) is more favorable than process (1) as will be discussed in Subsection III C.

C. PL intensity variations due to different ion beams and fluences

Since the sensitivity of quantum sensing and metrology is directly related to the density of NV centers, we systematically clarified the effects of ion irradiation conditions (ion species and fluences) on the PL intensity from NV centers. Figure 7 shows the irradiation fluence dependence of PL integrated intensity (1150–1450 nm) with different ion beams (240 keV-H, 2 MeV-N, 4 MeV-Si, and 7 MeV-I ions), measured at RT through 1064 nm excitation. The same trend was observed in the PL measurement at 80 K. These ion beams induced similar vacancy profiles, as shown in Fig. 1, and NV centers were thought to be mainly formed at the depth of 1.5–2 μm from the surface after thermal annealing. When focusing on the N-4H-SiC samples, the highest PL integrated intensity appeared at the intermediate fluence in all the cases, and the peak value was enhanced with increasing atomic mass of ion beams (I > Si > N > H). The highest PL integrated intensity was obtained using 7 MeV-I irradiation at 6.0×10^{12} cm^{-2}. Vacancy concentration increases with increasing irradiation fluence and also the amount of NV centers formed after thermal annealing increases. If an excess amount of vacancies is introduced by irradiation, however, sufficient recovery of the crystallinity is not expected even after thermal annealing. This results in the reduction of NV center formation and/or quenching of NV centers due to neighboring defects. In addition, the effects of implanted atoms as well as induced defects have to be considered when the irradiation fluence is high. According to the TRIM calculation, hydrogen concentration after the 240 keV-H irradiation at the fluence of 1.0×10^{16} cm^{-2} reaches 7.5×10^{20} cm^{-3} at the Bragg peak. Most of the residual implanted hydrogen is thought to be desorbed after thermal annealing at above 700 °C even though Si–H and C–H bonds were once formed.[49] We believe that the effects of H-related defects on NIR-PL properties are not significant, since no unique NIR-PL spectrum appeared from 240 keV-H irradiated samples compared to other irradiation conditions. No NIR-PL properties for H-related defects in SiCs have previously been reported to our knowledge. However, the possibility that a portion of implanted hydrogens form thermally stable complex defects after thermal annealing up to 1100 °C cannot be excluded.

To gain further insight into the relationship between the NV center formation and the radiation induced defects, the abscissa in Fig. 7 was rescaled by the amount of vacancies induced by irradiations. The number of vacancies induced by single ion beams was estimated by TRIM calculation[35] and the product of fluence and number of vacancies was defined as vacancies per area (cm^{-2}). Figure 8 shows the PL integrated intensity of N-4H-SiC samples as a function of vacancies per area. It is plausible that all the regions in which vacancies were induced by irradiations were observed in the measurement system of this study, since the ideal axial resolution of measurement system was estimated to be more than 5 μm when the refractive index of SiC is 2.6.[50] The result shows that the highest PL integrated intensity appeared at around 10^{17} vacancies cm^{-2} independent of ion species, indicating that the amount of NV center formation was determined by the amount of vacancies induced. The PL intensity was rather reduced above around 10^{17} vacancies cm^{-2}. Radiation damage studies have clarified that the critical dose of SiC for amorphization was about 0.2 dpa (displacement per atom) at RT,[51,52] although the critical dose also depends on ion species, ion energy, and irradiation temperature. The value of 0.2 dpa roughly

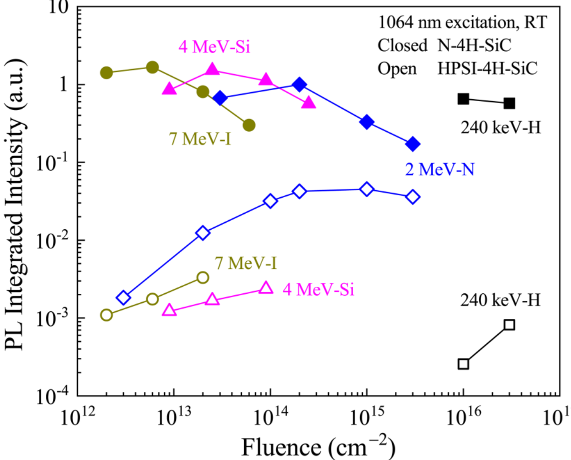

FIG. 7. PL integrated intensity (1150–1450 nm) at RT of N- and HPSI-4H-SiCs irradiated with different ions. The excitation wavelength was 1064 nm. Closed and open symbols denote the results of N- and HPSI-4H-SiCs, respectively. Squares in black: 240 keV-H, diamonds in blue: 2 MeV-N, triangles in pink: 4 MeV-Si, and circles in dark yellow: 7 MeV-Si irradiations. Thermal annealing of 1000 °C for 30 min in Ar atmosphere was performed after irradiation. The ordinate is normalized by the value of N-4H-SiC at 2.0×10^{14} cm^{-2}.

Published under license by AIP Publishing.

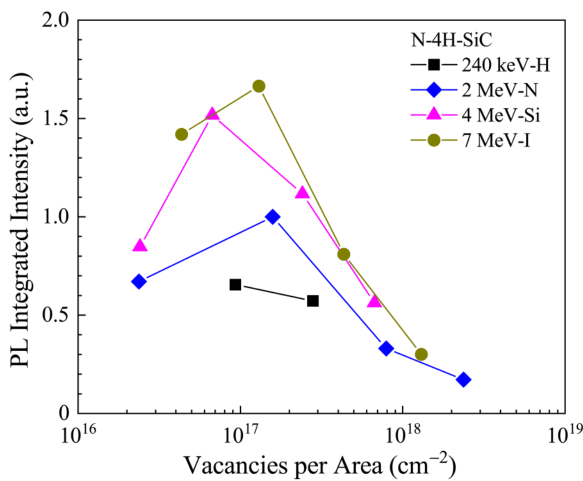

FIG. 8. PL integrated intensity of the N-4H-SiC samples as a function of vacancies per area (cm^{-2}), estimated by TRIM calculation.

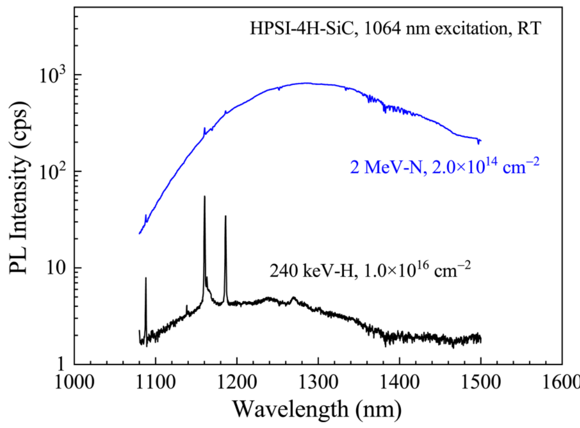

FIG. 9. PL spectra of the HPSI-4H-SiCs irradiated with 240 keV-H at 1.0×10^{16} cm^{-2} (black) and 2 MeV-N at 2.0×10^{14} cm^{-2} (blue) at RT. Observed four sharp peaks are attributable to the Raman scattering (see text).

corresponds to around 10^{18} vacancies cm^{-2} in this study and thus the reduction of PL intensity at above 10^{17} vacancies cm^{-2} is related to the appearance of amorphization. Since the (local) amorphization occurred at above 10^{17} vacancies cm^{-2}, the NV center formation was suppressed by the insufficient recovery of SiC lattice structure after the thermal annealing at 1000 °C. Regarding the correlation between the peak PL intensity and the atomic mass of ion beams, cascade damage by heavy ions is seemingly related to the enhancement of PL intensity. This can be explained by considering the defect kinetics as follows. According to Gerstmann *et al.*,[44] process (2) is more favorable than process (1) because of the lower activation energies. In process (2), more defects (I_C, V_C, and V_{Si}) are required than the process (1), and thus the cascade damage (localized dense defect region) has the potential to form NV centers effectively.

When focusing on the 2 MeV-N irradiations, the highest PL integrated intensity appeared at the fluences of 2.0×10^{14} cm^{-2} in the N-4H-SiC and 1.0×10^{15} cm^{-2} in the HPSI-4H-SiC. In the case of HPSI-4H-SiC, the peak might appear at the fluence between 2.0×10^{14} cm^{-2} and 1.0×10^{15} cm^{-2} as those values were fairly close. The fact that the PL intensity of HPSI-4H-SiC was drastically lower than that of N-4H-SiC (4.3% at 2.0×10^{14} cm^{-2}) indicates that the contained N atoms as impurities exclusively formed NV centers while the implanted N atoms less contributed to the NV center formation. The peak concentration of implanted N is estimated to be 1.2×10^{19} cm^{-3}, which is larger than the N-impurity concentration ([N] = 9×10^{18} cm^{-3}), and hence much higher PL intensity would have been observed in the HPSI-4H-SiC samples if the implanted N atoms had preferentially formed NV centers. This finding is also supported by the fact that in the peak PL intensities of N-4H-SiC irradiated with 4 MeV-Si and 7 MeV-I irradiations were higher than that of 2 MeV-N irradiation. This is probably because a thermal annealing temperature of 1000 °C is too low to diffuse implanted N atoms into lattice site ($N_I + V_C \rightarrow N_C$, where N_I the interstitial nitrogen) and NV centers are exclusively formed from N atoms in the lattice site. It cannot be excluded, however, that not $N_CV_{Si}^-$ centers (single negatively charge state) but $N_CV_{Si}^0$ centers (neutral state) were formed in the HPSI-4H-SiC samples because donors which could supply electrons were extremely low.

Nevertheless, implanted N atoms undoubtedly contribute to the NV center formation. As shown in Fig. 7, the NIR-PL integrated intensity of 2 MeV-N ion irradiated HPSI-4H-SiCs was much higher than the other HPSI-4H-SiCs. Figure 9 shows the PL spectra at RT of HPSI-4H-SiC samples irradiated with 2 MeV-N at 2.0×10^{14} cm^{-2} and 240 keV-H at 1.0×10^{16} cm^{-2}. Only extremely weak luminescence ranging from 1100 nm to 1400 nm appeared in the 240 keV-H irradiation even though the comparable amount of vacancies was introduced (see Fig. 1). Peaks observed at 1088.0 nm, 1160.2 nm, 1163.0 nm, and 1186.2 nm were assigned to be Raman scatterings of the E_2 PA, the E_2 PO, the E_1 transverse optical (TO), and the A_1 LO phonons, respectively.[39] This result strongly indicates that the NV centers formed in the HPSI samples were mainly originating from not a minute amount of N impurities but implanted N atoms. Therefore, we conclude that the NV centers were created from both implanted and contained N atoms after 1000 °C thermal annealing, although most of NV centers were created from contained N atoms. In addition, unlike the N-4H-SiC samples, the NIR-PL integrated intensity increased with increasing fluence in the ranges considered in this study. This implies that the N-impurity concentration strongly affects the NV center formation yields. Since these highest irradiation fluences were close to the critical dose of amorphization, further irradiation might reduce the NIR-PL intensity. Additional investigation is required to clarify the effects of impurity N concentration on the NV center formation.

Here, the creation yield of NV centers by N ion implantation is roughly estimated. The lowest PL integrated intensity was obtained from the HPSI-4H-SiC irradiated with 2 MeV-N at the fluence of 3.0×10^{12} cm^{-2}, although the plane distribution of PL intensity on the samples was also uniform. Taking into account that lateral resolution of the micro-PL measurement system was estimated

Published under license by AIP Publishing.

to be 0.60 μm (=$0.51 \times 1064/0.90$) when $\lambda = 1064$ nm and NA = 0.90 were used, this fact suggests that at least more than one NV center were formed within the area of 2.9×10^{-9} cm^2 on average. This value corresponds to the areal density of 3.5×10^8 cm^{-2}. Thus, the creation yield of NV centers by 2 MeV-N irradiation was estimated to be more than 0.012% (=$100 \times 3.5 \times 10^8/3.0 \times 10^{12}$) at least.

D. Temperature dependence on the PL intensity

Highly fluorescent PL signals are required at RT for applications of quantum sensors in the field of life science. In addition, high temperature operation of quantum sensors is also expected for applications in harsh environments like space.[34] Hence, temperature dependence on the PL intensity is one of the most important factors for their practical use as quantum sensors. The temperature dependence of the PL intensity originating from NV centers ranging from 80 K to 773 K is shown in Fig. 10. The N-4H-SiC irradiated with 7 MeV-I at 6.0×10^{12} cm^{-2} and the HPSI-4H-SiC irradiated with 2 MeV-N at 2.0×10^{14} cm^{-2} were measured. The abscissa is the reciprocal of temperature multiplied by 1000 and the ordinate is the PL integrated intensity from 1150 nm to 1450 nm normalized by the value of N-4H-SiC at 80 K. The PL intensities at RT and 683 K were reduced to be 75% and 9.8% for the N-4H-SiC and 94% and 29% for the HPSI-4H-SiC, respectively. The PL spectrum originating from NV centers was observed up to 773 K, which was the temperature limit of the measurement system. The same trend was obtained when the integrated range was from 1215 nm to 1235 nm where NV-ZPL at *hh* site appeared.

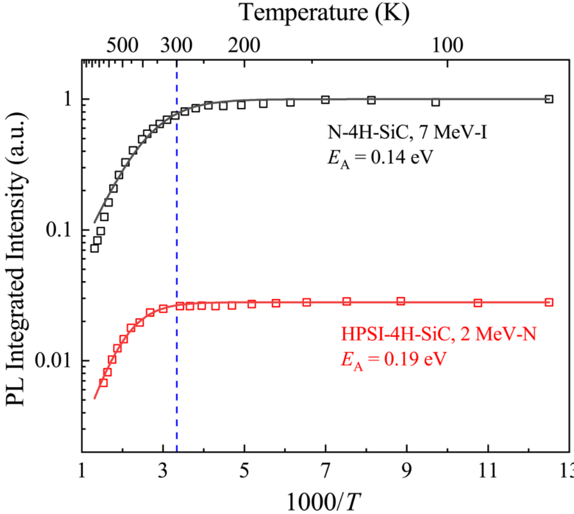

FIG. 10. PL integrated intensity (1150–1450 nm) as a function of temperature. Black squares and red circles denote the N-4H-SiC irradiated with 7 MeV-I at the fluence of 6.0×10^{12} cm^{-2} and the HPSI-4H-SiC irradiated with 2 MeV-N at 2.0×10^{14} cm^{-2}, respectively. Solid lines denote the fitting results by Eq. (1). Thermal annealing of 1000 °C for 30 min in Ar atmosphere was performed after irradiation. The excitation wavelength was 1064 nm. The abscissa is the reciprocal of temperature multiplied by 1000 and the ordinate is the PL integrated intensity normalized by the value of the N-4H-SiC at 80 K. The vertical dashed line in blue shows RT (300 K).

Temperature dependence of PL intensity can be generally expressed as the following equation:

$$I \propto \frac{1}{1 + A \exp\left(-\frac{E_A}{k_B T}\right)}, \tag{1}$$

where I, T, k_B, E_A, and A are the PL intensity, the temperature, the Boltzmann constant, the activation energy of thermal quenching, and the fitting constant, respectively. The experimental results were well fitted by Eq. (1) (solid lines in Fig. 10) and the activation energy was obtained to be 0.14 eV in the N-4H-SiC and 0.19 eV in the HPSI-4H-SiC. Carrier escape and/or energy transfer from NV centers to other neighboring defects are thought to be the cause of thermal quenching. These values might be related to the difference of energy levels between the excited state of NV centers and the other defects which act as recombination centers. V_{Si} and V_C are one of the candidates for the cause of thermal quenching, since their excited levels are located at about 0.2 eV above the excited levels in NV centers.[26]

IV. CONCLUSIONS

We studied PL properties of NV centers in 4H-SiCs, which were irradiated with various conditions and were then thermally annealed at different temperatures. The effect of excitation wavelengths, power densities, and temperatures on PL properties was systematically investigated and the following conclusions were obtained.

It was shown from the results of the temperature dependence of PL spectra that the broad spectrum ranging from 1100 nm to 1500 nm at RT is attributable to the PL from NV centers. NV center ZPLs were clearly evident when studied at a temperature of 80 K. The PL from NV centers mainly appeared by 1064 nm excitation in both the N- and HPSI-4H-SiC samples, whereas the PL from V_{Si}^-s and VVs also appeared through 785 nm excitation in the HPSI-4H-SiC samples. NV centers are preferentially formed rather than VVs in the N-4H-SiC samples and the PL from VVs were not significantly observed at 80 K even by 1064 nm excitation, since the formation energy of NV centers are lower than that of VVs In addition, it was shown from the results of laser power density dependence that the NV centers were more efficiently excited at 1064 nm than 785 nm. This is because the absorption energy of NV centers is close to the photon energy of 1064 nm (1.165 eV). It was shown from the thermal annealing temperature dependence that the optimal temperature for creating NV enters was around 1000 °C. It would appear the NV center formation is rather suppressed at above 1000 °C due to the formation of other types of N-related complex defects. Comparing the PL intensities among different ion irradiation conditions under the same amount of radiation induced defects, the heavier ion irradiation provides more effective NV center formation than the lighter ion irradiation. This suggests that the cascade damage effectively contributes to NV center formation. It was also clarified that NV centers were mainly formed from contained N atoms as impurities rather than implanted N atoms.

Published under license by AIP Publishing.

The results of temperature dependence of PL intensities show the weak thermal quenching property, unlike the PL from VVs The PL intensities at RT were comparable to that at 80 K in both the N- and HPSI-4H-SiC samples, and the PL from NV centers appeared even at 773 K. Considering this fact, in combination with the other reports on the spin properties based on EPR (electron paramagnetic resonance) studies,[31] quantum sensing using NIR-PL from NV centers in SiC operating at RT (or even high temperature), which is desirable for life science and space applications, is highly feasible.

ACKNOWLEDGMENTS

This study was supported by the JSPS KAKENHI under Grant No. 17H01056. The authors would like to thank Professors Brant C. Gibson and Andrew D. Greentree of RMIT University for their fruitful discussion.

REFERENCES

[1] T. D. Ladd, F. Jelezko, R. Laflamme, Y. Nakamura, C. Monroe, and J. L. O'Brien, Nature **464**(7285), 45–53 (2010).
[2] J. R. Weber, W. F. Koehl, J. B. Varley, A. Janotti, B. B. Buckley, C. G. Van de Walle, and D. D. Awschalom, Proc. Natl. Acad. Sci. U.S.A. **107**(19), 8513–8518 (2010).
[3] J. Wrachtrup and F. Jelezko, J. Phys. Condens. Mat. **18**(21), S807–S824 (2006).
[4] A. Boretti, L. Rosa, A. Mackie, and S. Castelletto, Adv. Opt. Mater. **3**(8), 1012–1033 (2015).
[5] J. Jeske, J. H. Cole, and A. D. Greentree, New J. Phys. **18**(1), 013015 (2016).
[6] T. Wolf, P. Neumann, K. Nakamura, H. Sumiya, T. Ohshima, J. Isoya, and J. Wrachtrup, Phys. Rev. X **5**(4), 041001 (2015).
[7] V. M. Acosta, E. Bauch, M. P. Ledbetter, C. Santori, K. M. C. Fu, P. E. Barclay, R. G. Beausoleil, H. Linget, J. F. Roch, F. Treussart, S. Chemerisov, W. Gawlik, and D. Budker, Phys. Rev. B **80**(11), 115202 (2009).
[8] G. Kucsko, P. C. Maurer, N. Y. Yao, M. Kubo, H. J. Noh, P. K. Lo, H. Park, and M. D. Lukin, Nature **500**(7460), 54–58 (2013).
[9] A. Gruber, A. Dräbenstedt, C. Tietz, L. Fleury, J. Wrachtrup, and C. Von Borczyskowski, Science **276**(5321), 2012–2014 (1997).
[10] M. W. Doherty, N. B. Manson, P. Delaney, F. Jelezko, J. Wrachtrup, and L. C. L. Hollenberg, Phys. Rep. **528**(1), 1–45 (2013).
[11] L. Gordon, A. Janotti, and C. G. Van de Walle, Phys. Rev. B **92**(4), 045208 (2015).
[12] H. Kraus, V. A. Soltamov, F. Fuchs, D. Simin, A. Sperlich, P. G. Baranov, G. V. Astakhov, and V. Dyakonov, Sci. Rep. **4**, 5303 (2014).
[13] S. A. Tarasenko, A. V. Poshakinskiy, D. Simin, V. A. Soltamov, E. N. Mokhov, P. G. Baranov, V. Dyakonov, and G. V. Astakhov, Phys. Status Solidi (b) **255**(1), 1870101 (2018).
[14] V. Ivády, J. Davidsson, N. T. Son, T. Ohshima, I. A. Abrikosov, and A. Gali, Phys. Rev. B **96**(16), 161114(R) (2017).
[15] A. Lohrmann, T. J. Karle, V. K. Sewani, A. Laucht, M. Bosi, M. Negri, S. Castelletto, S. Prawer, J. C. McCallum, and B. C. Johnson, ACS Photonics **4**(3), 462–468 (2017).
[16] H. Kraus, D. Simin, C. Kasper, Y. Suda, S. Kawabata, W. Kada, T. Honda, Y. Hijikata, T. Ohshima, V. Dyakonov, and G. V. Astakhov, Nano Lett. **17**(5), 2865–2870 (2017).
[17] F. Fuchs, B. Stender, M. Trupke, D. Simin, J. Pflaum, V. Dyakonov, and G. V. Astakhov, Nat. Commun. **6**, 7578 (2015).
[18] M. Widmann, S. Y. Lee, T. Rendler, N. T. Son, H. Fedder, S. Paik, L. P. Yang, N. Zhao, S. Yang, I. Booker, A. Denisenko, M. Jamali, S. A. Momenzadeh, I. Gerhardt, T. Ohshima, A. Gali, E. Janzen, and J. Wrachtrup, Nat. Mater. **14**(2), 164–168 (2015).
[19] G. Wolfowicz, C. P. Anderson, A. L. Yeats, S. J. Whiteley, J. Niklas, O. G. Poluektov, F. J. Heremans, and D. D. Awschalom, Nat. Commun. **8**(1), 1876 (2017).
[20] C. F. de las Casas, D. J. Christle, J. Ul Hassan, T. Ohshima, N. T. Son, and D. D. Awschalom, Appl. Phys. Lett. **111**(26), 262403 (2017).
[21] D. J. Christle, P. V. Klimov, C. F. de las Casas, K. Szász, V. Ivády, V. Jokubavicius, J. Ul Hassan, M. Syväjärvi, W. F. Koehl, T. Ohshima, N. T. Son, E. Janzén, Á Gali, and D. D. Awschalom, Phys. Rev. X **7** (2), 021046 (2017).
[22] D. J. Christle, A. L. Falk, P. Andrich, P. V. Klimov, J. U. Hassan, N. T. Son, E. Janzen, T. Ohshima, and D. D. Awschalom, Nat. Mater. **14**(2), 160–163 (2015).
[23] A. L. Falk, B. B. Buckley, G. Calusine, W. F. Koehl, V. V. Dobrovitski, A. Politi, C. A. Zorman, P. X. Feng, and D. D. Awschalom, Nat. Commun. **4**, 1819 (2013).
[24] A. L. Falk, P. V. Klimov, B. B. Buckley, V. Ivady, I. A. Abrikosov, G. Calusine, W. F. Koehl, A. Gali, and D. D. Awschalom, Phys. Rev. Lett. **112**(18), 187601 (2014).
[25] W. F. Koehl, B. B. Buckley, F. J. Heremans, G. Calusine, and D. D. Awschalom, Nature **479**(7371), 84–87 (2011).
[26] B. Magnusson, N. T. Son, A. Csóré, A. Gällström, T. Ohshima, A. Gali, and I. G. Ivanov, Phys. Rev. B **98**(19), 195202 (2018).
[27] A. Csóré, H. J. von Bardeleben, J. L. Cantin, and A. Gali, Phys. Rev. B **96**(8), 085204 (2017).
[28] H. J. von Bardeleben, J. L. Cantin, A. Csóré, A. Gali, E. Rauls, and U. Gerstmann, Phys. Rev. B **94**(12), 121202(R) (2016).
[29] S. A. Zargaleh, B. Eble, S. Hameau, J. L. Cantin, L. Legrand, M. Bernard, F. Margaillan, J. S. Lauret, J. F. Roch, H. J. von Bardeleben, E. Rauls, U. Gerstmann, and F. Treussart, Phys. Rev. B **94**(6), 060102(R) (2016).
[30] S. A. Zargaleh, S. Hameau, B. Eble, F. Margaillan, H. J. von Bardeleben, J. L. Cantin, and W. Gao, Phys. Rev. B **98**(16), 165203 (2018).
[31] H. J. von Bardeleben, J. L. Cantin, E. Rauls, and U. Gerstmann, Phys. Rev. B **92**(6), 064104 (2015).
[32] R. R. Anderson and J. A. Parrish, J. Invest. Dermatol. **77**(1), 13–19 (1981).
[33] A. M. Smith, M. C. Mancini, and S. Nie, Nat. Nanotechnol. **4**, 710–711 (2009).
[34] C. J. Cochrane, J. Blacksberg, M. A. Anders, and P. M. Lenahan, Sci. Rep. **6**, 37077 (2016).
[35] J. F. Ziegler, M. D. Ziegler, and J. P. Biersack, Nucl. Instrum. Meth. B **268**(11–12), 1818–1823 (2010).
[36] J. W. Steeds, G. A. Evans, L. R. Danks, S. Furkert, W. Voegeli, M. M. Ismail, and F. Carosella, Diamond Relat. Mater. **11**(12), 1923–1945 (2002).
[37] A. L. Barry, B. Lehmann, D. Fritsch, and D. Braunig, IEEE Trans. Nucl. Sci. **38**(6), 1111–1115 (1991).
[38] J. Lefèvre, J.-M. Costantini, S. Esnouf, and G. Petite, J. Appl. Phys. **105**(2), 023520 (2009).
[39] J. C. Burton, L. Sun, M. Pophristic, S. J. Lukacs, F. H. Long, Z. C. Feng, and I. T. Ferguson, J. Appl. Phys. **84**(11), 6268–6273 (1998).
[40] M. Chafai, A. Jaouhari, A. Torres, R. Antón, E. Martı´n, J. Jiménez, and W. C. Mitchel, J. Appl. Phys. **90**(10), 5211–5215 (2001).
[41] S. Nakashima, T. Kitamura, T. Mitani, H. Okumura, M. Katsuno, and N. Ohtani, Phys. Rev. B **76**(24), 245208 (2007).
[42] J. S. Embley, J. S. Colton, K. G. Miller, M. A. Morris, M. Meehan, S. L. Crossen, B. D. Weaver, E. R. Glaser, and S. G. Carter, Phys. Rev. B **95**(4), 045206 (2017).
[43] X. Wang, M. Zhao, H. Bu, H. Zhang, X. He, and A. Wang, J. Appl. Phys. **114**(19), 194305 (2013).
[44] U. Gerstmann, E. Rauls, T. Frauenheim, and H. Overhof, Phys. Rev. B **67**(20), 205202 (2003).
[45] D. A. Golter and C. W. Lai, Sci. Rep. **7**(1), 13406 (2017).
[46] K. Danno and T. Kimoto, J. Appl. Phys. **100**(11), 113728 (2006).
[47] G. Alfieri, E. V. Monakhov, B. G. Svensson, and M. K. Linnarsson, J. Appl. Phys. **98**(4), 043518 (2005).
[48] M. Bockstedte, A. Mattausch, and O. Pankratov, Phys. Rev. B **69**(23), 235202 (2004).
[49] T. Seyller, R. Graupner, N. Sieber, K. V. Emtsev, L. Ley, A. Tadich, J. D. Riley, and R. C. G. Leckey, Phys. Rev. B **71**(24), 245333 (2005).
[50] P. T. Shaffer, Appl. Opt. **10**(5), 1034–1036 (1971).
[51] W. Jiang, Y. Zhang, and W. J. Weber, Phys. Rev. B **70**(16), 165208 (2004).
[52] L. B. Bayu Aji, T. T. Li, J. B. Wallace, and S. O. Kucheyev, J. Appl. Phys. **121**(23), 235106 (2017).

Published under license by AIP Publishing.